High Density High Performance Plasma with Internal Diffusion Barrier in Large Helical Device

R. Sakamoto, M. Kobayashi, J. Miyazawa, S. Ohdachi, T. Morisaki, S. Masuzaki, I. Yamada, M. Goto, K. Ida, S. Morita, S. Sakakibara, K. Tanaka, K.Y. Watanabe, Y. Suzuki, H. Funaba, N. Ashikawa, Y. Nagayama, Y. Narushima, B.J. Peterson, M. Shoji, C. Suzuki, M. Tokitani, S. Yoshimura, N. Ohyabu, H. Yamada, A. Komori, O. Motojima and LHD experimental group

National Institute for Fusion Science, Toki, Japan

e-mail contact of main author: sakamoto@LHD.nifs.ac.jp

Abstract. A attractive high density plasma operational regime, namely an internal diffusion barrier (IDB), has been discovered in the intrinsic helical divertor configuration on the Large Helical Device (LHD). The IDB which enables core plasma to access a high density/high pressure regime has been developed. It is revealed that the IDB is reproducibly formed by pellet fueling in the magnetic configurations shifted outward in major radius. Attainable central plasma density exceeds 1×10^{21} m^{-3}. Central pressure reaches 1.5 times atmospheric pressure and the central β value becomes fairly high even at high magnetic field, i.e. $\beta(0) = 5.5\%$ at $B_t = 2.57$ T.

1. Introduction

The internal diffusion barrier (IDB) which enables core plasma to access high-density/high-pressure regime was found in multi pellets fueled high density discharges with an actively pumped local island divertor (LID) configuration in large helical device (LHD) [1]. A high density core plasma with 5×10^{20} m^{-3} is maintained by the IDB located around $\rho = 0.5$ and the IDB plasma exhibits the highest fusion triple product on LHD. The IDB has similarity to pellet enhanced performance (PEP) mode, which is first found in JET[2] then in the other tokamaks [3, 4], on the point that both lead to strongly peaked pressure profile. On the other hand, unlike the tokamak PEP mode, there is no clear indication of increase in the temperature gradient and inward particle convection in IDB. Although the LID configuration has efficient pumping due to the localized installation, heat removal is a problem for the same reason with the present LID design. Therefore, IDB formation in intrinsic helical divertor configuration which has larger heat receiving area than LID configuration is highly desired from a standpoint of compatibility with a fusion reactor. An experimental study has been performed in order to explore the operational space of the IDB discharge with the intrinsic helical divertor configuration in LHD.

2. Experimental Setup

LHD is a heliotron-type full superconducting device with a pair of continuous helical coils and three pairs of poloidal coils. The position of the magnetic axis for the vacuum magnetic field (preset magnetic axis R_{ax}) is variable in the range of 3.5 m to 4.1 m, and the magnetic axis position is an essential parameter characterizing configuration effect in LHD. The averaged plasma minor radius a is ∼ 0.6 m and the magnetic field strength is ≤ 3 T[5]. A helical divertor is intrinsic divertor configuration in a heliotron type device. The divertor has open structure with forced water-cooled carbon target plates and there is no pumping capacity except wall pumping. Three negative ion based high energy (up to 180 keV) neutral beam injectors (NBI), which are injected tangentially with respect to the LHD, are employed for plasma heating. Typical NBI

heating power is 12 MW in total in this study. Solid hydrogen ice pellets are launched from the outboard side mid-plane by using *in-situ* pipe-gun pellet injector[6] which can inject 10 pellets per plasma discharge at preset timing. The typical pellet mass and velocity are $1.5 - 2.0 \times 10^{21}$ hydrogen atoms per pellet and 1000-1200 m/s, respectively.

3. Result

3.1. Effects of Fueling on IDB Formation

Core fueling by multi-pellet injection is absolutely essential for IDB formation. An IDB is formed in a density decay phase after intensive core fueling by multiple pellet injections at 35 - 50 ms intervals. Once developed IDB structure is maintained even after central density decrease down to half. Typical profiles of the gas-puff and pellet fueled discharges at the same central electron temperature T_e = 1 keV under the similar discharge conditions are shown in FIG. 1. The plasma profiles are plotted in flux coordinates and real-space coordinates. In the case of gas-puff fueled high density plasma, the densify profile typically become hollow because particle source is limited to the peripheral. On the other hand, the IDB which has a steep density gradient inside $\rho \approx 0.5$ is formed and the central density is remarkably increased while the peripheral density is reduced in the case of pellet fueling. A noteworthy finding is that the central electron density of the pellet fueled plasma is about five times higher than that of gas puff fueled plasma. Therefore, the plasma pressure profile of the pellet fueled IDB plasma shows an obvious increase of the plasma energy density in the core region. The central plasma pressure exceeds atmospheric pressure and the central $\beta(0)$ become 4.4 % even at 2.54 T. The IDB plasma profile is characterized by very large Shafranov shift due to the peaked high pressure and it reach half the radius ($a_{\rm eff}/2 \approx 0.3$ m).
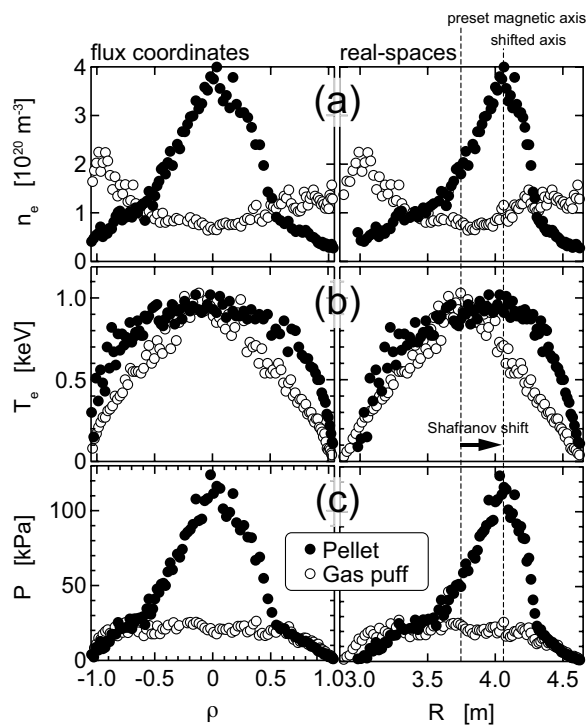

FIG. 1. Profile comparison of (a) electron density, (b) electron temperature and (c) plasma pressure in the gas-puff (open circle) and pellet (filled circle) fueled discharges at the same magnetic configuration $R_{\rm ax}$ = 3.75 m. The profiles are shown in the flux coordinates (left-hand side) and real-space coordinates(right-hand side).

3.2. Effects of Magnetic Configuration (R_{ax}) on IDB formation

The global energy confinement time reaches a maximum in inward shifted magnetic configurations ($R_{ax} = 3.60 - 3.65$ m) which give a maximum plasma volume by employing pellet fueling[7]. An IDB is reproducibly developed in the magnetic configuration with the outward shifted magnetic axis ($R_{ax} > 3.7$ m). A mechanism of the magnetic axis dependence has yet to be revealed, but the outward shifted configurations have the following characteristics: magneto-hydrodynamically stable[8] because the region with magnetic well is wide especially at finite β, larger helical ripple transport, lower equilibrium limit, more efficient central heating due to geometry of LHD neutral beam injection system.

FIG. 2 shows the temporal evolution of characteristic plasma parameters, namely (a) central electron density $n_e(0)$, (b) central electron temperature $T_e(0)$, (c) central plasma pressure $P(0)$ and (d) collisionality inside IDB ν_b^* which is electron-electron collision frequency normalized to the bounce frequency of banana particles, in nine-pellet fueled discharges at preset magnetic axes $R_{ax} = 3.65$ m, 3.75 m and 3.85 m. Abscissa is a time, which is measured with respect to the time of the maximum density. In each case, NB heating power and magnetic strength are 12 MW and 2.54 T, respectively. The IDB formation period, which is temporarily defined here by existence of a sharp bend in the density profile, is denoted by filled symbol. The IDB profile gradually changes in time. While the same number of pellets were injected, attainable central plasma density becomes higher as the preset magnetic axis position is put outwards. The maximum central density with $R_{ax} = 3.85$ m doubles compared to one with $R_{ax} = 3.65$ m. At the same time, central temperatures decrease with injecting pellets and the temperatures drop down to around 300 eV after multi pellets injection sequence independently of the preset magnetic axis position. It is an interesting result that the central temperature change during the pellets injection and subsequent recovery phases follow quite a similar course although the central density varies widely depending on magnetic axis position. As the result, higher central pressure is attainable in the outward shifted magnetic configurations where the IDB is formed. The point to observe is that there is a slackened growth state of the pressure rise in the high density phase as shown by two-headed arrows in FIG. 2(c). The slackened growth state begins to appear during the pellet injection sequence, namely density increase phase, and continues until the excess densities drops to the onset levels. This phenomena give the appearance that confinement degradation in high density regime. As the preset magnetic axis position is put outward, the onset density level increase as indicated by broken line in FIG. 2(a), namely 2.5×10^{20} m^{-3} at $R_{ax} = 3.65$ m and 5.0×10^{20} m^{-3} at $R_{ax} = 3.75$ m. The slackened growth state of the pressure rise is hardly observed at $R_{ax} = 3.85$ m and the pressure is increase in a linear fashion during and after pellet injection. After that, the pressure and density decrease suddenly at $t = 0.18$ s, while any noticeable changes are not observed in the central temperature. This unexpected event is referred to as core density collapse (CDC) event[9]. It must be also noted that the decay rate of the central density after reaching the maximum pressure increase as the preset magnetic axis position is put outward, and therefore the final density after disappearance of the IDB becomes lower as the preset magnetic axis position is put outward. These observations suggest a change of particle transport property during IDB formation period. As for particle transport property of the IDB plasma, we will take up in **3.3.**.

FIG. 3 shows comparison of electron density profiles at the time of the maximum pressure in $R_{ax} = 3.65$ m, 3.75 m and 3.85 m. In spite of the same discharge conditions other than preset magnetic axis position, obtainable density profiles differ substantially. As for $R_{ax} = 3.65$ m in which IDB cannot be formed, density profile shows monotonous parabolic distribution. On the other hand, there is a sharp bend which separate the density profile into the low density mantle
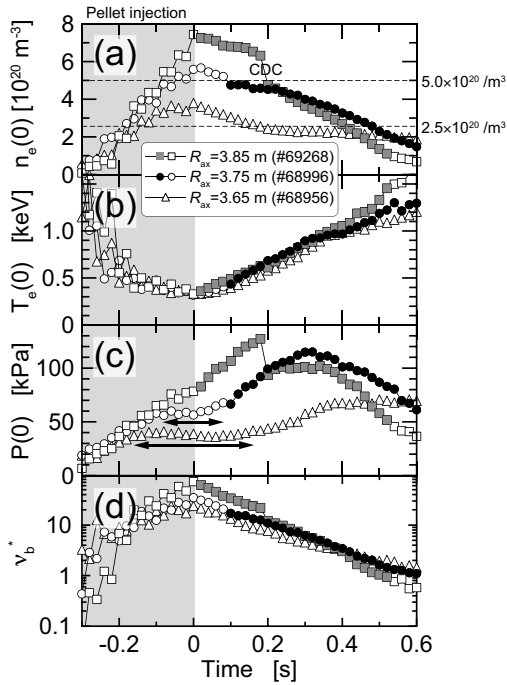
FIG. 2. *Temporal evolution of (a) central electron density, (b) central electron temperature, (c) central plasma pressure and (d) collisionality in nine-pellets fueled discharges at magnetic axes R_{ax} = 3.65 m (triangle), 3.75 m (circle) and 3.85 m (square). The magnetic field strength and NB heating power are 2.54 T and 12 MW, respectively. Filled symbols denote the IDB formation period.*
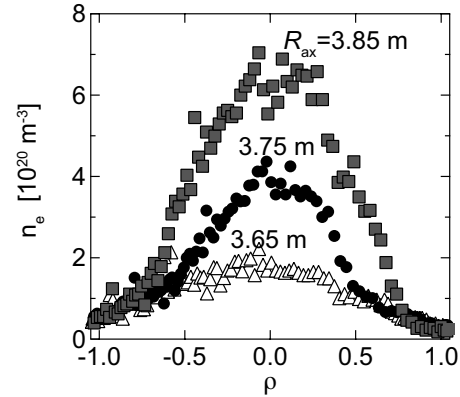
FIG. 3. *Comparison of electron density profile among R_{ax} = 3.65 m (triangle), 3.75 m (filled circle) and 3.85 m (filled square) at the timing of maximum pressure. The magnetic field strength and NB heating power are 2.54 T and 12 MW, respectively.*

and high density core region in the case of R_{ax} = 3.75 m and 3.85 m. The IDB foot, namely, the position of the sharp bend in the density profile is located in $\rho \approx 0.5$ and 0.8 at R_{ax} = 3.75 m and 3.85 m, respectively. The central density is quite different due to IDB formation, but on the other hand, a mantle density do not depend on the preset magnetic axis. Thus magnetic configuration is another factor of the IDB formation in addition to pellet core fueling.

The preset magnetic axis position dependence is summarized in FIG. 4 (a) Shafranov shift and IDB foot position, (b) maximum central density and (c) maximum central pressure with fixed heating power P_{NB} = 12 MW and magnetic field strength B_T = 2.54 T. The Shafranov shift reach to half the radius in the IDB Discharges R_{ax} > 3.7 m. The IDB foot point widens outwardly as the magnetic axis becomes outward, and the IDB foot reaches to the last closed flux surface at R_{ax} = 4.0 m. Attainable central density $n_e(0)$ becomes higher as the preset magnetic axis is put outward. The maximum attained density exceeds 1×10^{21} m^{-3} at R_{ax} = 3.9 m and above. The point to observe is that there is a sharp increase in central pressure between R_{ax} = 3.7 m and 3.75 m. The central pressure reach its largest value $\sim$ 130 kPa at the neighborhood of R_{ax} = 3.85 m. The central pressure rise is limited by CDC event in which the high density core plasma is expelled on the sub millisecond time scale without having impact on the central temperature. The mechanism of the CDC event has not yet been elucidated, but it may be involved with MHD instability and/or the equilibrium limit arising from a very large Shafranov shift. In order to suppress such an unfavorable event, mitigation of Shafranov shift by using ellipticity κ control (Pfirsch-Schlüter current suppression by a vertical elongation) is shown to be effective. As the κ become large, the Shafranov shift reduces and the attainable
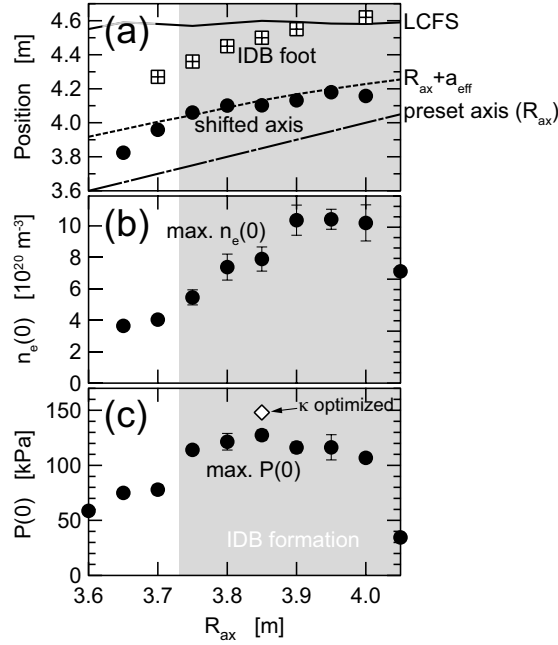
FIG. 4. Preset magnetic axis position dependence of the (a) Shafranov shift and IDB foot position, (b)maximum central density and (c) maximum central pressure. The magnetic field strength and NB heating power are fixed at 2.54 T and 12 MW, respectively.

central pressure, which is restricted by a CDC event, is become large until $\kappa = 1.2$. The attainable central pressure increase by 20 % compare to standard configuration $\kappa = 1.0$ and reaches its largest value $P(0) = 150$ kPa ($\beta(0) = 5.5\%$ at 2.57T) as shown by open diamond in FIG. 4(c).

3.3.   Particle Transport Property of IDB Plasmas

FIG. 5 shows a change of IDB profiles with $R_{ax} = 3.75$ m at representative times, namely, immediate aftermath of pellet injection sequence ($t = 0$ s), time of the maximum pressure ($t = 0.3$ s) and just before disappearance of IDB ($t = 0.5$ s), where $t = 0$ is defined by termination time of multi pellet injection sequence. At the immediate aftermath of pellet injection sequence, linear density profile without IDB and flat temperature profiles are observed. The central density and temperature are 4.0×10^{20} m^{-3} and 300 eV, respectively. At the time of the maximum pressure, density outside of $R = 4.3$ m decrease by half of one at $t = 0$ s while keeping high central density 4.0×10^{20} m^{-3}. Such a difference in the density decay rate between core and mantle plasma cause IDB formation. In addition to this, the central temperature recovers about 3 times as compared to one at $t = 0$ s. These facts lead to high density/high pressure plasma. Then central density is gradually decreases while keeping mantle density. The IDB structure is maintained even after central density decreases down to half and the central pressure is kept by increasing temperature until $t = 0.5$ s. During IDB formation period, the IDB foot point hardly moves despite the significant changes of the density and temperature. During the profile change, a collisionality ν_b^*, which is electron-electron collision frequency normalized to the bounce frequency of banana particles, decreases monotonically in the plateau regime ($10 \geq \nu_b^* \geq 1$) as shown by filled circle in FIG. 2(d).

The particle transport coefficient of IDB plasma is calculated by using relationship between time evolution and gradient of density profiles after pellet injection. FIG. 6 shows a flux-gradient diagram, i.e. relationship between normalized particle flux Γ_e/n_e and normalized density gradient

$-(dn_e/d\rho)/n_e$. Gradient and y-intercept of the flux-gradient diagram indicate diffusivity (D_e) and convection velocity (v_e) according to the following relational expression.

$$\frac{\Gamma_e}{n_e} = -\frac{D_e}{a}\frac{1}{n_e}\frac{\partial n_e}{\partial \rho} + v_e,$$

where $\Gamma_e = -\frac{1}{A}\int\frac{\partial n_e}{\partial t}dV$ is particle flux assuming no particle source inside the flux surface. The filled and open symbols denote the IDB formation period and relatively low density period after disappearance of IDB, respectively. The normalized density gradient inside IDB ($\rho \leq 0.5$) increases as time advances just after pellet injection sequence due to the mantle density decrease while keeping up the core density (phase **a**). Then, the normalized flux increases without the normalized density gradient change around the time when the the central pressure reaches maximum (phase **b**). In the final phase of the IDB period, the normalized density gradient decreases monotonously as the central density decay and the IDB structure disappears (phase **c**). The diffusivities, which are estimated by gradient of the diagram, inside IDB in both phases **a** and **c** are kept at low level as $D_e = 0.05 \pm 0.01$ m²/s even high density gradient. The point to observe is that there is an offset in the normalized flux during the phase **c** and this indicates the existence of outward convection velocity about $v_e = 0.2$ m/s. In terms of the phase **b**, diffusivity and convection velocity can not be determined by the relationship between the normalized particle flux and normalized density gradient due to transient state. Since the diffusivity is quite unlikely to change drastically only for a short period of time between two phases **a** and **c**, it is satisfactory to consider the convection velocity change gradually while keeping constant diffusivity during phase **b**. On the other hand, the particle transport of the mantle plasma is obviously different from one of the core plasma and the mantle plasma cannot keep the density gradient in high particle flux IDB phase (phase **A**). The flux-gradient diagram indicates about 10 times larger diffusivity as $D_e = 0.43 \pm 0.08$ m²/s than one of the core plasma. Then, the gradient of the flux-gradient diagram becomes gentle and it is merge into the phase **c**
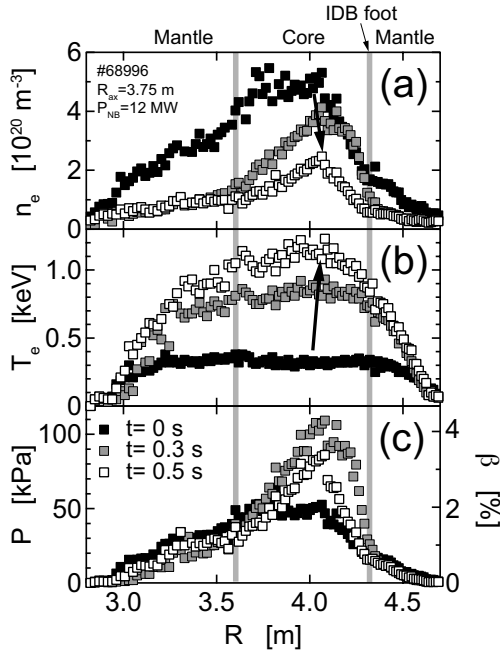

FIG. 5. Profile change of (a) electron density, (b) electron temperature and (c) plasma pressure at representative times.
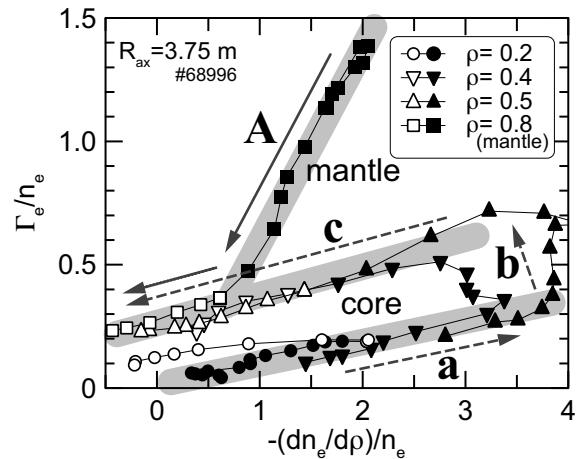
FIG. 6. Particle flux normalized by electron density as a function of density gradient after pellet injection in various minor radius. Filled symbols denote the period of IDB formation and open symbol denote the state of no-IDB.
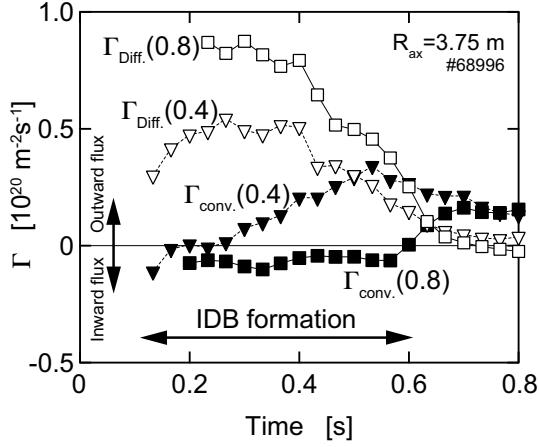
FIG. 7. *Temporal change of the diffusion component* $-\frac{D_e}{a}\frac{\partial n_e}{\partial \rho}$ *and convection component* $n_e v_e$ *of the particle flux at core (ρ = 0.4) and mantle (ρ = 0.8).*
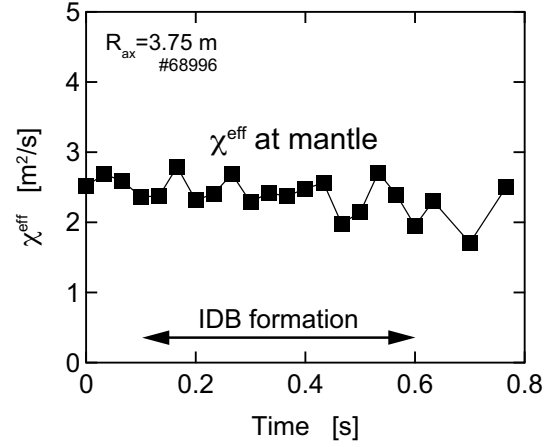
FIG. 8. *Temporal change of the thermal transport coefficient* χ^{eff} *at mantle.*

of the core plasma after disappearance of the IDB structure. FIG. 7 shows the temporal evolution of the diffusion components $-\frac{D_e}{a}\frac{\partial n_e}{\partial \rho}$ and convection components $n_e v_e$ of the particle flux at mantle (ρ = 0.8) and inside IDB (ρ = 0.4). These fluxes are calculated by supposing a constant core diffusivity and large mantle diffusivity during IDB formation period as noted above. In the mantle plasma, diffusion component of the particle flux dominates particle transport during IDB formation period due to large diffusivity and near-zero convection. As decreases the density, the diffusion component is reduced gradually and the particle transport dominator switches with the convection component after disappearance of IDB (t > 0.6 s). In the core plasma, diffusion component also dominates particle transport just after pellet core fueling. However, convection component increases as time advances and it goes beyond the diffusion component before disappearance of IDB. Therefore, an increase of the density decay rate after reaching the maximum pressure is explained by increase of the convection velocity. Notable characteristics of the IDB plasma is that the thermal transport coefficient χ^{eff}, which is evaluated using an one-dimensional transport code for helical plasmas, PROCTR[10] by assuming $T_i = T_e$ and $n_i = n_e$, remain unaffected by big change of the particle transport as shown in FIG. 8. These results lead to separation of confinement region between the IDB core (high density gradient) and low density mantle (high temperature gradient), and therefore high-density/high-pressure plasma is attained in the IDB discharge. The IDB core is formed by the deep pellet fueling and intrinsic good particle confinement property. The low density mantle has advantages to suppress radiation loss, and therefore density limit of IDB plasma is extremely extend to high-density regime. In addition, low density mantle secure temperature gradient for high-density/high-pressure core plasma.

4.   Discussions and conclusions

The experimental fact suggests advantage of the outward shifted magnetic axis configuration (R_{ax} > 3.75 m) to obtain high density/high pressure plasma. However, this result was not necessarily mean difference of the particle confinement property among the magnetic configuration. Lack of the neutral beam heating penetration may explain the preset magnetic axis dependence of the attainable density. It must be noted that the minimum central temperature is not less than 0.3 keV independently of the preset magnetic axis, neutral beam heating power and central density. Under such low temperature conditions, injected pellets pass through the plasma

cross section before the ablation is over and the central electron density shows no effective increase with subsequent pellet injections. A neutral beam power deposit calculation by using FIT code[12] indicates that central heat deposition becomes inhibited as the density increases in general, and this tendency is particularly true for inward shifted magnetic axis configuration. This result suggests that the minimum temperature which is required to ablate the solid hydrogen pellet is not kept due to lack of an effective central heating power in inward shifted magnetic axis configuration, and therefore high density operation is not available. The experimental fact that the attainable density decreases when the neutral beam heating power is reduced can be also explained by the lack of effective central heating power. The attainable central density is directly related to the central heating power. If the central heating is available even in the inward shifted magnetic axis configuration in which excellent global confinement property is provided, further extension of the operational space is expected.

An experimental study is performed to explore the operational space of a high density plasmas due to the IDB which was originally found in pellet fueled high density discharges with the actively pump LID configuration in LHD. The IDB with steep density gradient has been reproduced in an intrinsic helical divertor configuration as in LID configuration by optimizing the pellet fueling and magnetic configuration. Core fueling by multiple pellet injection is essential for the IDB formation. Confinement region is separated into low density mantle and high density core in IDB plasma. This lead to high-density/high-pressure core plasma. The central density reaches 1×10^{21} m^{-3} at $R_{ax} \geq 3.9$ m and the central pressure has reached 1.5 times atmospheric pressure. CDC event, which occurs at very large Shafranov shift, restrict operational regime. Suppression of Shafranof shift with ellipticity control can mitigate CDC event and the central pressure increase by 20 % of standard configuration.

Investigation of long-duration sustainability of the pellet fueled IDB is critically important from a perspective of extrapolation to fusion reactor scenario. Nonetheless, the IDB encourages alternative path for fusion ignition scenario, high-density/low-temperature ignition approach in helical devices.

References

[1] N. OHYABU *et al.*, Phys. Rev. Lett. **97**, 055002 (2006).
[2] JET TEAM, Plasma Phys. Control. Fusion **30**, 1467 (1988).
[3] Y. TAKASE *et al.*, Phys. Plasmas **4**, 1647 (1997).
[4] L.R. BYLOR *et al.*, Phys. Plasmas **7**, 1878 (2000).
[5] O. MOTOJIMA *et al.*, Phys. Plasmas **6**, 1843 (1999).
[6] H. YAMADA *et al.*, Fusion Eng. Des. **49-50**, 915 (2000).
[7] R. SAKAMOTO *et al.*, Nucl. Fusion **41**, 381 (2001).
[8] H. YAMADA *et al.*, Plasma Phys. Controlled Fusion **43**, A55 (2001).
[9] H. YAMADA *et al.*, Plasma Phys. Controlled Fusion **49**, B487 (2007).
[10] H.C. HOWE, ORNL/TM-11521 (1990).
[11] M. KOBAYASHI*et al.*, Plasma and Fusion Res. **3**, S1005 (2008).
[12] S. MURAKAMI *et al.*, J. Plasma and Fusion Res. Ser. **2**, 255 (1999).